HHS Public Access

Author manuscript

Nat Aging. Author manuscript; available in PMC 2022 June 04.

Published in final edited form as:

Nat Aging. 2021 December ; 1(12): 1148–1161. doi:10.1038/s43587-021-00143-2.

Regulation of aged skeletal muscle regeneration by circulating extracellular vesicles

Amrita Sahu[1,2], **Zachary J. Clemens**[2], **Sunita N. Shinde**[1], **Sruthi Sivakumar**[1,3], **Abish Pius**[1,4], **Ankit Bhatia**[5], **Silvia Picciolini**[6], **Cristiano Carlomagno**[6], **Alice Gualerzi**[6], **Marzia Bedoni**[6], **Bennett Van Houten**[7], **Mita Lovalekar**[8], **Nicholas F. Fitz**[2], **Iliya Lefterov**[2], **Aaron Barchowsky**[2,7], **Radosveta Koldamova**[2], **Fabrisia Ambrosio**[1,2,3,9,*]

[1]Department of Physical Medicine & Rehabilitation, University of Pittsburgh, Pittsburgh, PA

[2]Department of Environmental and Occupational Health, University of Pittsburgh, Pittsburgh, PA

[3]Department of Bioengineering, University of Pittsburgh, Pittsburgh, PA

[4]Department of Computational & Systems Biology, School of Medicine, University of Pittsburgh, Pittsburgh PA

[5]Robotics Institute, Carnegie Mellon University, Pittsburgh, PA

[6]Laboratory of Nanomedicine and Clinical Biophotonics (LABION), IRCCS Fondazione Don Carlo Gnocchi, Milan, Italy

[7]Department of Pharmacology and Chemical Biology, University of Pittsburgh, Pittsburgh, PA

[8]Department of Sports Medicine and Nutrition, School of Health and Rehabilitation Sciences, University of Pittsburgh, Pittsburgh PA

[9]McGowan Institute for Regenerative Medicine, University of Pittsburgh, Pittsburgh, PA

Abstract

Heterochronic blood exchange (HBE) has demonstrated that circulating factors restore youthful features to aged tissues. However, the systemic mediators of those rejuvenating effects remain poorly defined. We show here that the beneficial effect of young blood on aged muscle regeneration was diminished when serum was depleted of extracellular vesicles (EVs). Whereas EVs from young animals rejuvenate aged cell bioenergetics and skeletal muscle regeneration,

[*]**To whom correspondence should be addressed:** Fabrisia Ambrosio, PhD, MPT, Suite 308, Bridgeside Point Building II, 450 Technology Drive, Pittsburgh, PA 15219, Phone: 412-624-5276, ambrosiof@upmc.edu.

Author contributions

F.A. and A.S. provided the concept, idea and experimental design for the studies. F.A. and A.S. wrote the manuscript. A.S., Z.J.C., S.S., S.N.S., and A.P. provided data collection, analyses, interpretation and review of the manuscript. An.B. provided computer-vision and machine-learning based analyses. S.P., C.C., A.G. provided data collection and analyses. M.B. provided data interpretation and manuscript review. B.V.H. provided data analysis, interpretation and manuscript review. Aa.B. provided consultation with data interpretation and review of the manuscript. M.L. provided support with statistical analyses. N.F., I.L. and R.K. provided support with data interpretation. F.A. provided funding for the studies.

CODE AVAILABILITY

The code used to perform machine learning based analyses on EVs are uploaded on https://github.com/ankitbhatia/bioimage_aging. To generate PCAs the OriginLab plugin called “Principal Component Analysis for Spectroscopy” was used. The code for RNAseq analysis is available on https://github.com/sruthi-hub/Aging_EV/tree/main.

Competing interests: The authors declare that they have no competing interests.

aging shifts EV subpopulation heterogeneity and compromises downstream benefits on recipient cells. Machine learning classifiers revealed that aging shifts the nucleic acid, but not protein, fingerprint of circulating EVs. Alterations in sub-population heterogeneity were accompanied by declines in transcript levels of the pro-longevity protein, α-Klotho, and injection of EVs improved muscle regeneration in a Klotho mRNA-dependent manner. These studies demonstrate that EVs play a key role in the rejuvenating effects of HBE and that Klotho transcripts within EVs phenocopy the effects of young serum on aged skeletal muscle.

Editor summary:

Circulating factors play an important role in tissue aging. Here, the authors show that serum extracellular vesicle (EV) sub-populations and cargoes remodel with age, and that EVs from young mouse serum rejuvenate aged skeletal muscle.

INTRODUCTION

Circulating factors play crucial roles in regulating tissue homeostasis and organismal aging. One approach to identify the effects these circulating factors have on target tissues involves the surgical joining of a young and an old mouse, or heterochronic parabiosis. Heterochronic parabiosis couples the circulatory systems of the two animals such that the aged parabiont is exposed to circulatory factors from the young parabiont, and vice versa.[1] This model has provided valuable insight into the influence of age-associated humoral factors on function of stem cells and tissues, including skeletal muscle.[2–6]

Whereas studies investigating mechanisms underlying the beneficial effect of heterochronic parabiosis on aged tissue function have primarily focused on free circulating proteins, a growing number of findings have demonstrated that a large portion of the circulating secretome is packaged within membranous nanoparticles, or extracellular vesicles (EVs). EVs traffic between anatomically remote sites and serve as couriers of proteins and genetic material.[7,8] EVs have been identified in most bodily fluids including plasma, serum, urine, saliva, and cerebrospinal fluid,[8–14] and emerging evidence suggests that mRNA cargoes within EVs can target and reprogram cells in a range of tissues to regulate physiological functions or pathophysiological processes.[15] Given their potent role in intercellular communication, it is not surprising that age-related alterations in EV structure and content have been increasingly associated with pathologies of aging.[16–19] However, whether circulating EVs mediate the “rejuvenating” effects of heterochronic parabiosis on skeletal muscle regeneration has not been investigated.

Here, we evaluate the contribution of circulating EVs on the beneficial effect of young serum on aged muscle stem cells and the skeletal muscle regenerative cascade. We show that young serum restores a youthful bioenergetic and myogenic profile to aged muscle cell progeny, and that this effect is dependent on the presence of circulating EVs. Moreover, whereas youthful EV cargoes preserve mitochondrial ultrastructure and respiration in target muscle cells, aged EV cargoes propagate mitochondrial dysfunction. *In vivo*, we confirmed previous reports demonstrating that young serum enhanced muscle regeneration, and we show that this benefit is diminished when the serum is depleted of EVs. These findings were

further supported by transcriptomic analysis, which revealed that the majority (61.5%) of differentially expressed genes altered in response to young serum are attributed to EVs. To better understand the effect of time on EV structure and cargoes, we employed machine learning classifiers to characterize changes in EV heterogeneity over time. The data revealed a shift in EV subpopulation dynamics that was concurrent with diminished nucleic acid content. Upon further interrogation, we found that EVs display an age-associated decrease in transcript levels of α-Klotho (Klotho), a longevity protein that has been positively associated with the maintenance of mitochondrial bioenergetics as well as skeletal muscle health.[20–22] Notably, we found that the impact of young EVs on muscle progenitor cell bioenergetics and myogenicity, as well as skeletal muscle regeneration, was dependent on the presence of Klotho mRNA. Together, these findings suggest that Klotho transcripts within circulating EVs contribute to the non-cell autonomous, systemic regulation of aged skeletal muscle regeneration.

RESULTS

EVs modulate cell bioenergetics in an age-dependent manner

Circulating factors are critical determinants of skeletal muscle regeneration, and previous studies have shown that exposure of aged muscle stem cells (MuSCs) to young serum *in vitro* increases myogenic potential.[2,3] Consistent with these previous reports,[2,3] we found that expression of MyoD, a master regulator of myogenesis,[23] and desmin, a muscle-specific intermediate filament, were increased in aged MuSC progeny (MPCs) cultured in the presence of young serum (Fig. 1a–c). Pax7, on the other hand, was significantly decreased in the presence of young serum (Extended DataFig. 1). Downregulation of Pax7 is necessary for myogenic lineage progression.[24]

Given that aberrant myogenic lineage specification of MuSCs has been shown to result from impaired mitochondrial function,[21,25,26] we also evaluated the impact of young versus aged serum on mitochondrial respiration. Aged MPCs cultured in the presence of young serum displayed a significantly increased basal oxygen consumption rate when compared to cells exposed to aged serum (Fig. 1d). Young serum also improved mitochondrial ultrastructure of aged progenitor cells, as demonstrated by a 1.5-fold increase in the reduced form of the mitochondrial inner membrane phospholipid, cardiolipin (Fig. 1e, f). Cardiolipin plays a key role in the maintenance of mitochondrial membrane integrity, as well as the modulation of oxidative phosphorylation.[27] These findings support the hypothesis that serum-derived components preserve target cell mitochondrial ultrastructure and bioenergetics in an age-dependent manner.

One mechanism through which serum-derived factors may affect mitochondrial quality control and activation of the metabolic machinery within recipient cells is via the transport of membrane-enclosed paracrine factors, EVs.[19] To determine whether EVs contribute to the observed effects of young serum on muscle progenitor cell myogenic profile and mitochondrial function, we depleted young and aged serum of EVs, and again performed immunofluorescence imaging of Pax7, MyoD, and desmin, together with live cell assessment of respiration (Fig. 1g–j, Supplemental Fig. 1a). NanoSight particle tracking analysis confirmed that treated serum was depleted of >95% of EVs (Supplemental Fig.

1a). Data revealed that the effect of young serum on cell proliferation, myogenicity, and bioenergetics was lost in the absence of circulating EVs (Fig. 1i, j, Supplemental Fig. 1b, c). Consistent with bioenergetic findings, MPCs treated with young serum displayed a gradual and progressive increase in the mitochondrial marker, succinate dehydrogenase sub-unit A (SDHA), over time, though the effect was blunted when cells were treated with aged serum or EV-depleted young serum (Supplemental Fig. 2a). SDHA is a major subunit of the succinate-ubiquinone oxidoreductase complex of the mitochondrial respiratory chain.[28] Our findings were not unique to myogenic progenitors, and we also found that depletion of EVs abrogated the beneficial effect of young serum on the bioenergetics of fibro-adipogenic progenitors (FAPs) (Supplemental Fig. 2b).

To confirm that the effect of EV depletion was not a result of toxicity resulting from the depletion protocol or coincident elution of serum proteins, another cohort of MPCs were co-cultured with young serum, young serum depleted of EVs, or depleted serum supplemented with column-isolated EVs (Supplemental Fig. 3). For this repletion study, we added an equivalent number of column-isolated EVs as we calculated to be removed during the depletion protocol (**see** Methods **for calculations**). EVs were isolated using size-exclusion chromatography, as per previous reports,[29] and purity of the EV population was confirmed by the presence of CD63 and CD81[30], as well as an absence of cytosolic contaminant, GM130 (Supplemental Fig. 4).[31] Repletion of the depleted serum with isolated EVs restored the beneficial effect of young serum on MyoD expression of target cells, suggesting that the depletion protocol does not induce cellular toxicity (Supplemental Fig. 3). Another group of cells were incubated with all components eluted during the Exo-Quick depletion protocol (i.e., EVs and other potentially undefined proteins). There was no difference in the myogenicity of cells treated with Exo-Quick precipitate versus isolated EVs (Supplemental Fig. 5), further supporting the hypothesis that the blunted myogenicity of cells treated with depleted serum is predominantly attributed to a loss of circulating EVs.

We next evaluated whether circulating EVs may contribute to the previously reported beneficial effects of young serum on skeletal muscle regeneration *in vivo*.[2,3] For this, aged mice received serial tail vein injections of young serum or young serum that was depleted of EVs, according to a previous protocol that evaluated the ability of young blood to reverse age-related cognitive declines (Fig. 2a)[32]. Three days post injury, we observed an EV-dependent increase in MyoD when animals received young serum injections (Supplemental Fig. 6a). By 11 days post injury, heterochronic blood exchange significantly enhanced skeletal muscle regeneration and functional recovery, as determined by myofiber cross-sectional area and *in situ* contractile testing, respectively (Fig. 2b–d). These findings are consistent with previous reports demonstrating an increased myofiber cross-sectional area and regeneration index when aged mice were parabiosed with young mouse counterparts.[2,3] However, the beneficial effect of young serum on muscle regenerative potential was lost in the absence of circulating EVs (Fig. 2b–d). We also probed mitochondrial responses to young circulating EVs by immunofluorescent staining of SDHA. We observed enhanced SDHA within regenerating myofibers (i.e., centrally nucleated myofibers) of mice receiving young serum treatment (Fig. 2e, f). However, the increased expression of SDHA was abrogated in the absence of EVs (Fig. 2e, f).

The above *in vivo* findings indicate that circulating EVs may be recruited to an injury site and participate in skeletal muscle regeneration. We therefore designed a subsequent set of experiments in injured aged animals to test this possibility. Young serum was depleted of EVs, as described above, after which time we repleted the serum with fluorescently labeled column-isolated EVs (at a concentration equal to the concentration that was removed during the depletion protocol). Three days after unilateral tibialis anterior (TA) injury, animals received a tail vein injection of serum with labeled EVs or saline injection alone. After another two days (i.e., five days post injury), bilateral TAs were imaged using a LiCor Odyssey Clx system. Both TAs in animals receiving serum injections displayed significantly higher levels of EVs when compared to saline controls, and the presence of labeled EVs was significantly higher in the injured TAs when compared to uninjured contralateral TAs (Fig. 2g, h). Moreover, the majority of donor EVs were co-localized with MyoD at the site of injury (Fig. 2i). These findings confirm accumulation of circulating EVs to the site of skeletal muscle injury and suggest preferential uptake by myogenic progenitors.

Aging shifts subpopulation heterogeneity of circulating EVs

The ability of young EVs to enhance skeletal muscle regeneration in aged mice implies that endogenously circulating EVs in aged animals do not effectively support the regenerative cascade. Therefore, we quantified age-related changes in EVs and their direct effect on target cell responses. Consistent with serum co-culture experiments described above, aged MPCs cultured in the presence of young, but not old, EVs displayed increased MyoD expression and mitochondrial cardiolipin content (Fig. 3a, b; Supplemental Fig. 6b–d). These findings suggest that EVs and/or EV cargoes are internalized by recipient progenitor cells to modulate cellular responses, but that functional communication is disrupted with aging.

The transfer of information between EVs and their target cells is mediated by a wide range of EV surface markers and cargoes, including cytosolic proteins, membrane proteins, mRNAs, noncoding RNAs, and even DNA.[7] To further probe age-associated changes in circulating EV structure and population heterogeneity, we profiled the population characteristics of young versus aged EVs. Nanoparticle tracking analysis using a NanoSight apparatus confirmed that the size of isolated EVs was between 30–200 nm in diameter (Fig. 3c), which falls within the size-range of small- to mid-sized EVs.[33] Aged serum yielded a significantly higher concentration of EVs when compared to young serum (Fig. 3c), consistent with a previous report.[19]

Whereas NanoSight provides bulk characterization of the size and concentration of all nanoparticles in the population, it does not allow for quantification and characterization of sub-populations. Therefore, we used multispectral imaging flow cytometry (IFC) as a means to classify circulating EVs according to differential expression of CD63 and CD81.[33] Custom computer vision algorithms were initially applied in order to eliminate debris and non-circular particles from the dataset (Fig. 3d). Machine learning was then employed in order to determine the accuracy with which surface marker heterogeneity and/or structural characteristics could be used to classify EVs according to age. A gradient-boosted decision tree classifier, which was chosen because of its ability to rank features according to their

information gain, resulted in a predictive accuracy of ~75% with a variance of < 0.0005. We found that CD63-associated features rose to the top as the most discriminative of age (Fig.3e). Indeed, aging creates a notable shift in subpopulation heterogeneity, and image analysis revealed a significant increase in CD63 intensity over time ($p<0.0001$; Fig. 3f). These findings were consistent with a previous report that evaluated CD63 using flow cytometry,[17] but are inconsistent with CD63 analyses of young and aged EVs as determined by western blotting analysis.[19] The discrepancy in the findings confirm previous reports of divergent subsets of nanoparticles analyzed depending on the method employed.[34] In addition, whereas previous studies using western blotting bulk analysis of the EV population revealed an age-related increase in CD81,[17] ImageStream analysis revealed that CD81 was significantly decreased in aged EVs ($p<0.0001$; Fig. 3g). However, we note that the absolute change in CD81 intensity was small, and, therefore, the physiological implications of these changes are unclear.

To better understand the impact of aging on internal EV cargoes that may underlie differential responses of target cells, we next performed Raman spectroscopy analysis of young and aged EVs. This method allows for bulk characterization of EV biochemical composition according to light scattering properties.[35] Qualitative EV differences as a function of age were evaluated by subtracting the aged EV spectra from the young, and the resulting Raman spectral peaks were assigned to functional chemical groups, as previously described.[36] Interestingly, there were no appreciable differences in the protein content of EVs according to age, which we further confirmed by a bicinchoninic acid assay (Fig. 3h, i, Supplemental Fig. 4b). However, aged EVs displayed a marked decrease (Δ Intensity > 0.2) in the Raman shift bands that are attributable to nucleic acids and a concomitant increase in lipid content. These findings suggest that aging may drive remodeling of EV genetic cargo and membrane composition, respectively. A hybrid model of unsupervised (Principal Component Analysis) and supervised (Linear Discriminant Analysis) dimension reduction techniques were then used to graphically express the differential variance of EVs according to age (Fig. 3j, k). Taken together, the label-free and non-invasive Raman fingerprints revealed a distinct biochemical profile of aged EV cargoes.

EVs dominate muscle transcriptomic responses to young blood

The data presented thus far suggest that aging alters EV composition and the transfer of mitochondrially-targeted information present in blood to recipient stem cell progeny. To better understand the response of injured skeletal muscle to circulating EVs at the level of the transcriptome, we repeated the serum injection protocol described above and performed RNA-seq analysis of hindlimb muscles in aged animals receiving tail vein injections of saline, young serum, or young serum depleted of EVs and evaluated muscles 11 days after injury (Fig. 4a). Linear Discriminant analysis (LDA) revealed that young serum and EV-depleted samples clustered separately from sham controls across the LD1 component, and young serum segregated from EV-depleted samples across LD2 (Fig. 4b). When we compared the differentially expressed genes (DEG) between young serum and sham versus young-depleted serum and sham, we found that the majority (313 genes; 61.5%) were dependent on the presence of EVs (Fig. 4c). Serum factors other than EVs accounted for 22.4% of the DEG (114 genes). A smaller group of genes (82 genes; 16.1%) were

exclusively altered when comparing young-depleted serum versus sham controls. These may indicate serum-related effects that are masked in the presence of EVs.

To investigate further the regulatory role of EVs in young serum on the transcriptomic profile of injured aged skeletal muscle, we enriched gene ontology (GO) terms associated with the 313 genes that were altered in the presence of EVs. Among the top altered processes, terms associated with the regulation of ion channels, and, specifically, calcium (Ca^{+2}) and potassium (K^{+}) predominated (Fig. 4d). Regulation of ion gradients is critical for mitochondrial health and function.[37–40]

Klotho transcripts are abundant in young, but not old, EVs

One candidate at the intersection of Ca^{2+}/K^{+} ion channel activity, mitochondrial function, and aging is the longevity protein Klotho[21,41–45]. Recent studies from our laboratory and other groups have shown that Klotho is necessary for the maintenance of MuSC mitochondrial function[21] and skeletal muscle regenerative capacity.[21,22,46] Upon activation, young MuSCs express and secrete higher levels of the Klotho protein than aged MuSCs, and loss of Klotho contributes to impaired MuSC mitochondrial ultrastructure and function over time.[21] Given the parallel effects of young serum EVs and Klotho protein, we tested whether EVs from young mice might contain positive regulators of Klotho expression in MuSCs and skeletal muscle, regulators that decline with age.

To evaluate the ability of EVs to induce Klotho expression in recipient cells, we cultured aged cells in the presence of EVs isolated from young serum or vehicle control. Immunofluorescence imaging revealed that Klotho protein in target cells was increased when aged cells were exposed to young EVs (Fig. 5a, b). ELISA analysis of conditioned media further demonstrated that cells cultured in the presence of young EVs displayed increased Klotho levels (Fig. 5c), suggesting that EVs also promoted Klotho secretion by recipient cells. In contrast, cells cultured with aged EVs displayed significantly lower Klotho protein levels when compared to cells cultured with young EVs (Extended Data Fig. 2).

As a more stringent test of whether EVs contain regulators of target MuSC Klotho expression, we tested the effect of EVs on MPCs isolated from Klotho-null (*Klotho*$^{-/-}$) mice. *Klotho*$^{-/-}$ MPCs cultured in the presence of young EVs displayed increased cytosolic and secreted Klotho protein levels (Fig. 5d, e, Supplemental Fig. 7). We note that the antibodies and ELISA kits used have been previously validated,[21,47] and the Klotho expression detected in the *Klotho*$^{-/-}$ cells and conditioned media are indicative of background signal. Given that *Klotho*$^{-/-}$ MuSCs lack a functional *Klotho* locus, these findings suggest that circulating EVs do not contain regulators that promote Klotho expression by target cells *per se*, but that EVs may deliver the Klotho protein directly to recipients.

In the light of these data, we next tested whether EVs store and transmit the Klotho protein and whether this information transfer changes with age. Whereas EVs within urine have been shown to contain Klotho protein[48], Klotho protein within serum-derived EVs has not to our knowledge been previously reported. Surface Plasmon Resonance imaging (SPRi) analysis revealed that circulating EVs contain Klotho protein. However, protein

levels were unaltered with aging (Fig. 5f). These findings, further confirmed using imaging flow cytometry (**Extended Data Fig. 5**), suggest that Klotho protein within EVs is not likely to explain the age-dependent ability of EVs to increase Klotho protein levels in target cells.

The Raman spectroscopy-based finding that aged EVs display a marked decline in nucleic acid content prompted us to next test whether the increase in Klotho protein by target muscle progenitors may be a result of the transfer of genetic information by EVs. EVs are capable of delivering mRNAs that are functional and capable of being translated in the target cells.[15] Specifically, transcripts within EVs can encode polypeptides to support protein synthesis and modulate cell responses.[15,49–51] To detect and quantify Klotho mRNA within peripheral EVs, we designed a set of Klotho oligonucleotides. Imaging flow cytometry revealed that young EVs contained abundant levels of Klotho mRNAs, but that Klotho mRNA content was significantly decreased in aged EVs ($p<0.0001$; Fig. 5g,h). We found that Klotho mRNA abundance was highly positively correlated with CD81 intensity ($R^2=0.90$; Supplemental Fig. 8). On the other hand, the correlation between Klotho transcript levels and CD63 was very low ($R^2=0.05$; Supplemental Fig. 8). These findings suggest that Klotho transcripts are selectively apportioned to a specific subset of circulating EVs. Given that the kidney is the primary source of Klotho,[52] we also probed for the podocyte kidney marker, podocin, in our EV populations. Unexpectedly, only 30% of EVs containing Klotho mRNA expressed podocin (Supplemental Fig. 9a), suggesting that the majority of these EVs may originate from alternate tissue sources.

To further confirm the age-dependent presence of Klotho transcripts within circulating EVs, we performed imaging flow cytometry to probe for Klotho mRNAs in circulating EVs of young and aged humans. As observed in mice, Klotho mRNAs in circulating EVs were decreased with increased age, though the difference between groups did not reach significance (Fig. 5i). Furthermore, RNAseq data of EVs isolated from the plasma of healthy individuals that was archived on Gene Expression Omnibus (GSE100206) database[53] revealed varying levels of Klotho transcripts, although ages of the individuals were not available (Fig. 5j, Supplemental Table 1).

To more directly test whether EV-derived Klotho mRNA is a source of Klotho protein within target cells, we tested whether treatment with a small interference RNA (siRNA) to Klotho would abate the Klotho response of recipient progenitors. After 48 hours of culture, we found that Klotho protein in aged muscle progenitors exposed to siRNA treated EVs was significantly lower than that from cells cultured in the presence of EVs treated with a scramble siRNA (Fig. 5k, Supplemental Fig. 7). Accordingly, inhibition of Klotho mRNA in young circulating EVs of a young animal also blunted the myogenic lineage progression of target aged MPCs, as determined by decreased MyoD and desmin expression. Inhibition of Klotho mRNA did not significantly affect the proliferative capacity of target cells, as evidenced by the number of ki67 positive cells (**Extended Data Fig. 5**). To rule out the possibility that the siRNA in EVs is transferred to the recipient cell where it inhibits endogenous Klotho, we again delivered young EVs +/− siRNA to muscle progenitor cells isolated from *Klotho*$^{-/-}$ mice. Just as was observed in wild type cells, the increased Klotho protein expression in *Klotho*$^{-/-}$ cells was blunted following treatment with siRNA (Fig. 5l; Supplemental Fig. 7).

To further demonstrate the ability of EVs to transfer Klotho transcripts to target cells and regulate mitochondrial integrity, we engineered EVs isolated from aged mice to carry Cy5-labeled synthetic Klotho mRNA. Co-culture of aged MPCs with engineered EVs confirmed that target cells take up and translate the EV-derived Klotho mRNA message, as evidenced by both an increased cytosolic Klotho protein and increased secreted Klotho within the conditioned media (Fig. 5m,n). Moreover, the increased Klotho protein in the target cells was concomitant with an enhanced mitochondrial ultrastructure, MyoD, and desmin (**Extended Data Fig. 5**). Proliferation of target cells was not significantly affected in the presence of synthetic Klotho mRNA (Fig. 5o, **Extended Data Fig. 5**). Together, these findings support the hypothesis that circulating EVs increase Klotho protein within target muscle cells via the transfer of Klotho mRNA and that this transfer supports target MPC mitochondrial integrity and myogenicity.

Next, we sought to evaluate the direct physiological contribution of circulating EVs on the skeletal muscle regenerative cascade *in vivo*. Aged mice were intramuscularly injected with EVs from young serum, EVs from aged serum, or a vehicle control (saline) at the site of an acute muscle injury (Fig. 6a). For these studies, we locally injected EVs so as to ensure a comparable number of donor EVs at the site of muscle injury across experimental groups (something not possible with systemic delivery). Injection of EVs derived from both young and aged mouse serum significantly enhanced myofiber cross sectional area when compared to saline-injected controls (Fig. 6b, c). However, there were significantly fewer regenerating fibers with aged serum EV treatment when compared to young serum EV-treated counterparts (Fig. 6d). Collagen I staining revealed that treatment with young serum EVs significantly decreased fibrotic deposition in the interstitial space when compared to treatment with saline or aged serum EVs (Fig. 6e, f). Histological evidence of improved myofiber regeneration in the presence of young, but not aged, EVs was supported by functional assessments, whereby aged muscle injected with young EVs displayed improved force recovery when compared to saline injected counterparts. However, the beneficial effect of EV injection on force recovery was lost when mice were injected with EVs isolated from the serum of aged mice (Fig. 6g).

To evaluate the extent to which the beneficial effect of young EVs on muscle regeneration is dependent on Klotho transcript levels, EVs were isolated from *Klotho*$^{+/-}$ animals and age-, sex, and strain-matched control mice. Imaging flow cytometry confirmed that EVs from *Klotho*$^{+/-}$ animals contained significantly reduced levels of Klotho mRNA (Supplemental Fig. 9b). Unexpectedly, Klotho protein was increased in the EVs of *Klotho*$^{+/-}$ animals that were characterized for EV markers, when compared to controls (Supplemental Fig. 9c–f). When we injected aged animals with equal numbers of EVs isolated from either the serum of young *Klotho*$^{+/-}$ animals or *Klotho*$^{+/+}$ controls, there was no difference in the mean cross-sectional area across groups (*Kl*$^{+/+}$ EVs: 1040± 279.6 μm^2, *Kl*$^{+/-}$ EVs: 810.8±157.2 μm^2, p=0.09). However, animals receiving *Klotho*$^{+/-}$ EVs displayed a significant decrease in the number of large myofibers (i.e., greater than 600 μm^2)[54], increased fibrosis, and impaired force recovery when compared to *Kl*$^{+/+}$ EV-injected controls (Fig. 7a–e). This impaired regenerative response in the presence of *Klotho*$^{+/-}$ EVs was concomitant with a decreased SDHA content in muscles injected with *Klotho*$^{+/-}$ EVs (Fig. 7f, Supplemental Fig. 9g). In

a subsequent gain-of-function rescue paradigm, we injected injured aged mice with young *Klotho*$^{+/-}$ EVs that were engineered to express synthetic Klotho mRNA. Restoration of Klotho mRNA levels resulted in a significantly improved myofiber cross-sectional area and reduced fibrosis when compared to animals treated with transfection-treated *Klotho*$^{+/-}$ EV controls (Fig. 7g–i). Moreover, SDHA content was significantly enhanced in the regenerating myofibers of muscles injected with engineered EVs (Fig. 7j,k). Taken together, these findings support the conclusion that Klotho transcripts within circulating EVs promote functional skeletal muscle regeneration.

DISCUSSION

The studies presented here demonstrate the anti-geronic effect of young circulating EVs on aged skeletal muscle regenerative potential. Prior studies have shown that muscle-derived EVs influence the myogenic profile of MuSCs.[55] However, the direct role of circulating EVs on the skeletal muscle regenerative cascade has not been studied. Transcriptomic profiling of muscles treated with young serum vs. young serum depleted of EVs suggest that most transcriptomic changes in aged muscle exposed to young serum are attributed to circulating EVs. Indeed, we found that young circulating EVs enhance mitochondrial function in MuSC progeny *in vitro* and functional skeletal muscle regeneration *in vivo*. Machine learning classifiers revealed that aging shifts EV subpopulation heterogeneity and a loss of EVs containing Klotho mRNA. Notably, we showed these transcripts to be preferentially apportioned to EVs expressing high levels of the surface marker, CD81 (CD81^{high}). Finally, we demonstrated that Klotho transcripts transferred from circulating EVs to recipient cells enhance target cell mitochondrial function *in vitro* and functional skeletal muscle regeneration *in vivo*.

To date, the bulk of studies investigating mechanisms underlying the beneficial effect of heterochronic blood exchange on aged tissues have primarily focused on identification of circulating proteins and their effects on a single tissue system of interest. As an alternative, here we tested the hypothesis that information stored within circulating EVs of young serum contains youthful signals that attenuate tissue aging. EVs are shed from cells by budding or by exocytosis, and the information contained within EVs (i.e. proteins, lipids, and genetic material) is a reflection of the originating cell health state.[7,8] This stored information within EVs is ultimately received and interpreted by a recipient cell to elicit a response. For example, EVs released from acutely stressed cells elicit a protective effect on recipient cells by making the recipient more tolerant to a future stressor stimulus.[56] In contrast, our results suggest that, under chronic conditions of stress such as aging, signals communicated by circulating EVs become less supportive—and potentially deleterious—in nature. Whereas young serum enhanced the mitochondrial ultrastructure and bioenergetics of aged muscle stem cell progeny, the benefit was lost when cells were cultured in serum depleted of EVs.

Although we focused here on the impact of aging and EVs on the bioenergetic responses of target MPCs, we also found that FAPs freshly isolated from aged muscle were similarly sensitive to the effect of EVs on mitochondrial function (Supplemental Fig. 2b). These findings suggest that the beneficial effect of young EV cargoes on target cell mitochondrial function may not be limited to muscle cells, though further studies are needed. Moreover,

the altered phenotype of MuSCs in the presence of young EVs is likely to trigger downstream effects on other resident muscle cell populations. Indeed, recent work by Fry et al, demonstrated that MPCs regulate collagen expression in FAPs via the exosome-mediated intercellular communication.[57]

Our finding that Klotho mRNA is preferentially stored in a population of CD81^{high} EVs is consistent with the current understanding that RNAs are actively apportioned to specific EV subpopulations.[58] In the context of miRNAs, for example, specific short motifs underlie selective sorting into exosomes (a subpopulation of EVs).[58] Further studies are needed to understand the cellular origin of Klotho mRNA within EVs, the mechanisms by which transcripts appear to be preferentially apportioned to CD81^{high} EVs, and how aging interferes with this sorting process. Finally, although Klotho protein has been previously shown to increase in activated MuSCs and is required for MuSC myogenic differentiation,[21] Klotho mRNA is likely just one amongst many age-dependent EV features that regulate MuSC function and skeletal muscle regeneration over time.

Taken together, these studies suggest that age-related declines in Klotho transcripts within circulating EVs may contribute to impaired mitochondrial function and regenerative response, but that exposure to young circulating EVs reverses this negative effect of time's arrow. We anticipate that an enhanced mechanistic understanding of the potential of circulating EVs to attenuate, prevent, or even reverse age-related declines in skeletal muscle regeneration may help pave the way towards the development of EV-based therapeutic approaches to the benefit of our growing geriatric population.

METHODS

Ethics approval, study design, and steps to ensure rigor

All animal experiments were performed with prior approval from the Institutional Animal Care and Use Committee of the University of Pittsburgh. We complied with all relevant guidelines set forth by the committee and the Division of Laboratory Animal Resources for all experiments. Additional details regarding age, sex, and genetic background of the mice used can be found in the supplemental file. For all *in vitro* and *in vivo* experiments, investigators performing endpoint analyses were blinded to the treatment group. *In vitro* studies were repeated in duplicate or triplicate on different days to ensure reproducibility. Only antibodies that have been validated were used. Source, product numbers, and lot numbers are available in the Supplemental file. For *in vivo* analyses, animals were ear-tagged and samples were number-coded. Animals with obvious health problems were eliminated prior to inclusion in the study. Animals in the lower and upper quartiles for either baseline performance or extent of injury were considered outliers, and, thus, removed prior to randomization (see Supplementary Fig. 10). All animals meeting criteria for inclusion were then randomized to treatment groups. *In vivo* studies included at least five animals per experimental group and were performed in two independent cohorts as possible (indicated in graphs are different colored data points and in the figure legends).

Serum collection and processing

Serum of young and aged C57/BL6 mice (obtained from Jackson laboratories and NIA Rodent colony, respectively), as well as *Klotho*$^{+/+}$, *Klotho*$^{+/-}$ and *Klotho*$^{-/-}$ mice (original breeders obtained from MMRCC, UC Davis) were isolated from blood obtained from animals using a cardiac puncture (see supplemental information for detailed methods).

In vitro experiments

Skeletal muscle progenitor cells and fibro-adipogenic progenitors were isolated from aged C57/BL6 (22–24 months) and/or Klotho$^{-/-}$ male mice (8 weeks), using a previously described protocol[21]. Cells were exposed to young or aged serum, with or without EVs for 48 hours, after which point endpoint analyses were performed.

Immunofluorescence imaging

Immunofluorescence staining for Klotho (R&D systems, MAB1819) and MyoD (SCBT, sc-760) as well as nonyl acridine orange (NAO) staining (Thermofisher, A1372) for cardolipin content was performed on aged cells across experimental groups. Muscle sections were analyzed for fiber cross-sectional area using an antibody against Laminin (Abcam, ab11575). Imaging was performed at 20X magnification on Zeiss-Axiovision microscope (see supplemental information for detailed methods).

Analysis of cellular bioenergetics

Oxygen consumption rate (OCR) was measured in real time using a Seahorse XFe96 Extracellular Flux Analyzer (Billerica, MA) as previously described.[59] Additional details provided in the supplemental file.

Serum injections in animals

Wild-type aged male C57/BL6 (21–24 months) were randomized into one of three cohorts that received tail-vein injections of 100 μL of young serum, 100 μL of young serum depleted of EVs, or sham injections. For studies of muscle function and transcriptomic analysis, animals were injected every three days for a total of eight injections.

Functional and histological analysis of muscle regeneration

For muscle function studies, on day 12 of serum injections experimental paradigm, aged male mice received injuries to bilateral Tibialis Anterior (TA) muscles via an intramuscular injection of cardiotoxin (10 μL of 1 mg/mL). Muscle function was evaluated on the 23rd day. To study the effect of EV injections on muscle regeneration after injury, three days post-injury, animals received 20–30 μL bilateral intramuscular injections of 5×10^8 – 7.5×10^8 EVs. *In situ* contractile testing was performed using a previously described protocol two weeks after injury[60]. TAs were harvested for histological analysis of myofiber regeneration using an antibody against Laminin. Myofiber cross-sectional area of centrally nucleated fibers (i.e., regenerating fibers) was quantified using ImageJ software, in which regenerating fibers were manually traced by a blinded investigator. All animals were randomly assigned to intervention group based on their baseline hang-impulse scores and were compared to age-matched littermate controls whenever possible (Supplemental Fig. 10).

EV isolation and characterization

EVs were isolated from serum of young, aged, Klotho$^{+/+}$ and Klotho$^{+/-}$ animals using size-exclusion chromatography (qEVsingle-35 nm iZON columns) according to manufacturer's instructions. The EVs collected in 6–11 fractions were characterized for size by Nanoparticle Tracking Analysis on NanoSight NS300. EVs were then characterized for CD63 (SCBT 5275) and CD81 (SCBT 23962) markers using multispectral flow cytometry-based ImageStream analysis.

Imaging-flow cytometry and computational analysis

EVs isolated from young and aged serum were analyzed using Amnis® ImageStream®XMark II - Luminex Corporation. Samples were stained for EV markers using conjugated antibodies: CD63 AF488, CD81 AF405, and a lipophilic dye, PKH26. A second set of samples were stained for PKH26, CD63 AF488, CD81 AF405 and Klotho mRNA. The PrimeFlow™ method for mRNA probing was performed according to the manufacturer's instructions (see supplemental document for detailed methods). A 20bDNAs mouse Klotho Type 1 oligos probe VB1–6001084 (Part No. 6003837) and mouse Klotho Type 10 oligo probe VB10–6001085 (Part No. 6003838) were hybridized with the label probes to evaluate total Klotho mRNA distribution within each EV (see supplemental methods for details). The fluorescent images for Klotho mRNA were captured using the 647 nm and 548 nm excitation laser of the instrument. Gating strategy employed for imaging both sets of samples of the EVs were based on a positive PKH26 signal as well as aspect ratio and particle area (Supplemental methods).

Both brightfield, side-scatter and fluorescent images of the EVs were captured using the INSPIRE® software. Classical computer vision-based algorithms in Python were applied to both, brightfield and side-scatter channels of each particle-image to filter out nanoparticles fitting the geometric criteria of EVs (for instance, high circularity). Statistical approaches and machine learning algorithms were applied to the filtered dataset to identify the best set of features that can accurately classify an EV into a particular age-group (see supplemental document for detailed methods).

SPR imaging and analysis

EVs were injected into the flow cell of the SPRi instrument XelPleX (Horiba Scientific SAS) over a gold chip (SPRi-Biochip, Palaiseau, France) onto which antibodies against Klotho were spotted using a micro-spotter (SPRi-Arrayer, Horiba). EzSuite software and OriginLab software were used to analyze the collected sensograms.

Raman Spectroscopy

Young and aged EVs isolated by size-exclusion chromatography were concentrated by an ultracentrifugation step (100,000 g × 70min). These EVs were then analyzed by means of Raman spectroscopy (LabRAM, Horiba Jobin Yvon S.A.S. Lille, France) following a previous published protocol[35].

ELISA

Media was collected from different sets of *in vitro* studies for ELISA based quantification of Klotho protein. For instance, aged MPCs were cultured at a concentration of 8,000 or 10,000 per well of an eight-well chamber slide in 250 μL volume, for 24 hours prior to any treatment condition. One billion EVs per well from different treatment groups were administered to the cells. Media was collected 48 hours after treatment. When cells were cultured on a 12-well tissue-culture treated plate, 20,000 cells were plated per well in a 500 μL volume, for 24 hours prior to any treatment condition. Two billion EVs were administered to the cells from different treatment groups and media was collected from the wells 48 hours post-treatment. Levels of Klotho protein in conditioned media were measured by a colorimetric sandwich enzyme immunoassay (SEH757Mu, Cloud-Clone Corp), according to manufacturer's instructions. The protein concentration was then normalized to total number of cells per well.

Engineering EVs to express synthetic Klotho mRNA

Aged EVs and Klotho$^{+/-}$ EVs were transfected with the synthetic Klotho mRNA oligonucleotides (Trilink Biotechnologies) using Exo-Fect™ Exosome Transfection Reagent from System Biosciences (Cat#EXFT-10A1). The loaded EVs were administered to aged MPCs for 48 hours. Refer to supplemental file for details.

Statistical analysis

Analyses were performed using GraphPad Prism version 8 software and IBM SPSS Statistics, Version 28 (IBM; Armonk, NY). Shapiro-Wilk and Levene's tests were initially performed to assess the normality of data and equality of variances, respectively. If assumptions of normality and homogeneity of variances were met, a Student's t-test was performed while comparing two groups. When conditions for normality were not met, the groups were compared using Mann-Whitney U test. A Welch's test was applied when there were differences between the standard deviations of the groups. For sample size less than 5, a non-parametric test was applied to compare the groups. Two-tailed tests were employed for all experiments comparing two groups. Any quantification comparing three experimental groups were analyzed by one-way ANOVA followed by Tukey's multiple comparison test or Dunn's multiple comparison test if test for normality was not met. For evaluating differences in force producing capacity between two groups across increasing frequencies, a two-way mixed ANOVA model was employed to evaluate the effect of frequency, experimental groups, and the interaction between them on specific force. All results were expressed as mean ± standard error. Statistical significance was set *a priori* at $p \leq 0.05$, two sided. Based on the preliminary investigations of peak muscle tetanic force in young and aged animals and after adjusting for unforeseen circumstances estimated at 20%, the final sample size for functional testing was 8–10 animals/group.

Extended Data

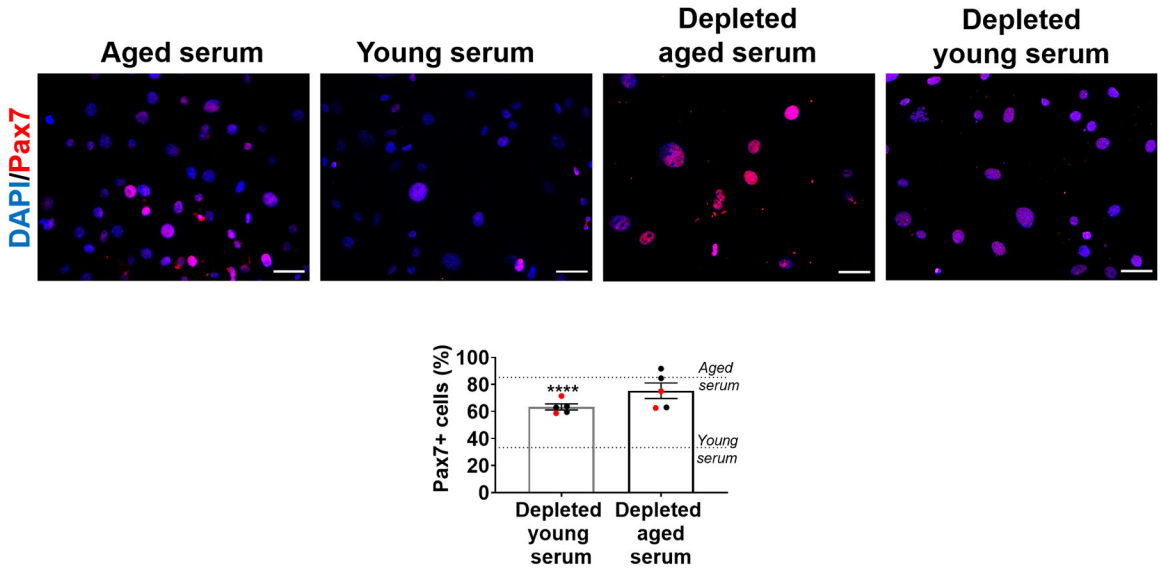

Extended Data Fig 1. Depletion of EVs eliminates the effect of young serum on Pax7 expression of muscle progenitors.

Quantification of Pax7+ in aged MPCs treated with aged serum, young serum, or EV-depleted aged or young serum. Scale: 50 μm. (****p<0.0001, two-tailed Mann-Whitney test comparing depleted young serum and young serum treatments). Data presented as mean ± SEM. Data from different cohorts or experimental groups performed on different days are presented within the same graph as black or red circles.

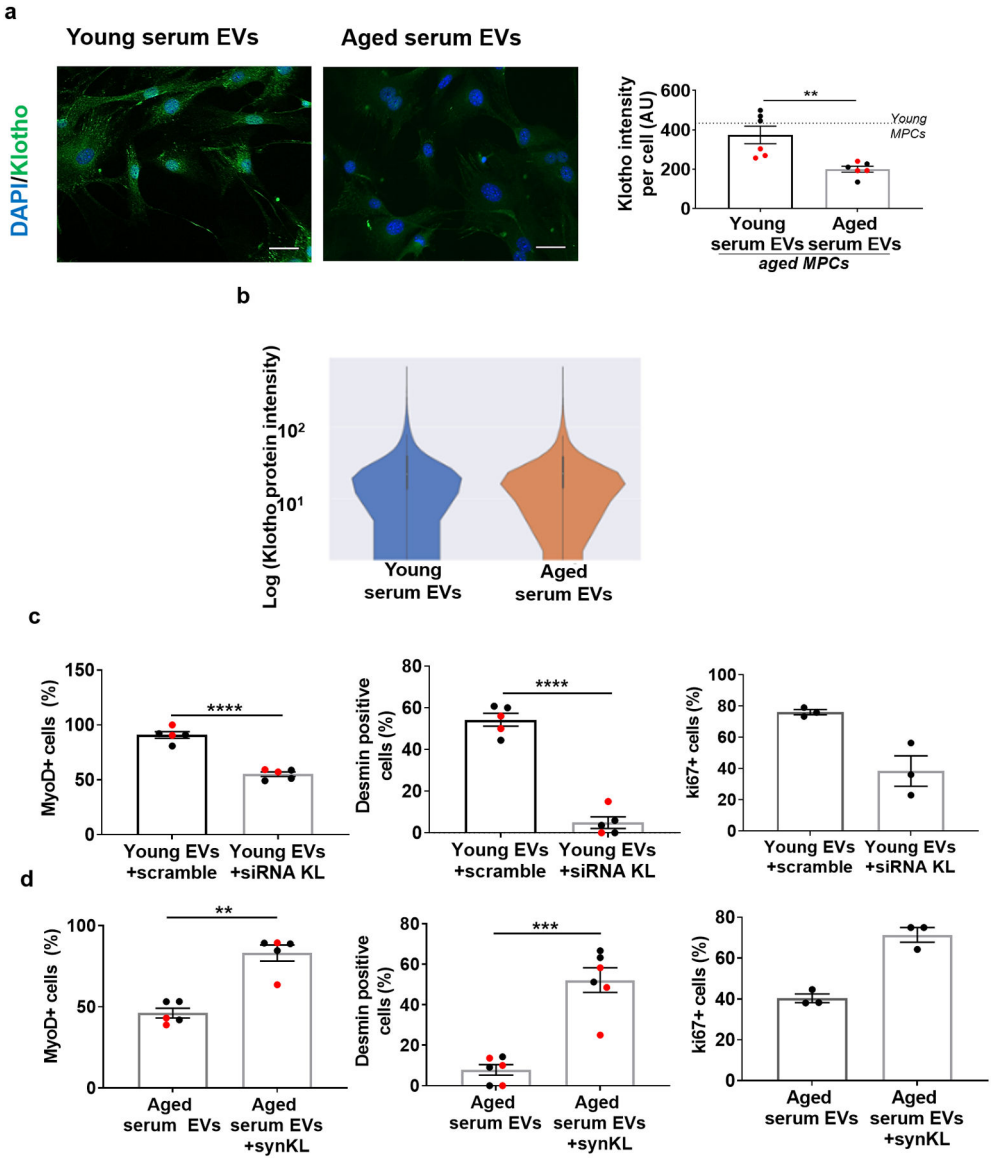

Extended Data Fig 2. The ability of EVs to modulate target cell Klotho and MyoD protein levels is dependent on Klotho mRNAs.

a, Imaging and quantification of Klotho protein in aged MPCs following culture in the presence of young or aged EVs for 24 hours. Scale: 50 μm.(n= 6 wells/group performed over two independent experiments, **p<0.01, two-tailed Welch's t-test). **b**, Representative violin plot of Klotho protein intensity per EV from young and aged serum, using imaging flow cytometry. (n=11,229–11,685 EVs/group for this experimental run. EVs pooled from 4 young and 4 aged serum samples, p>0.05, two-tailed Mann Whitney test, experiment repeated in triplicates). Violin plot minima, maxima, median, 25th percentile and 75th percentile are 0, 272915.9, 0, 0, and 26.36 for young, and 0, 272241.3, 0, 0, and 23.2 for aged respectively. **c,** Quantification of MyoD+ (%), desmin+ (%), and ki67+(%) aged MPCs receiving young serum EVs treated with scramble or siRNA to Klotho or **d,** aged serum EVs or aged serum EVs loaded with synthetic Klotho mRNA.(MyoD and desmin (scramble, siRNA), desmin (aged EVs, synKL): **p<0.01, ***p<0.001, ****p<0.0001,

two-tailed t-test with Welch's correction, n=5–6 wells/group; MyoD (aged EVs, synKL, **p<0.01, two-tailed Mann Whitney test, n=5 wells/group), ki67 (scramble, siRNA and aged EVs, synKL, p>0.05 (p=0.1), two-tailed Mann Whitney test). Data presented as mean ± SEM. Data from different cohorts or experimental groups performed on different days are presented within the same graph as black or red circles.

Supplementary Material

Refer to Web version on PubMed Central for supplementary material.

ACKNOWLEDGMENTS

These studies were supported by NIA R01AG052978 (FA), NIA R01AG061005 (FA), NIA R01AG066198-01 (FA and RK), R33 ES025606-05 (BVH), and UPMC Enterprises (FA). The authors also thank the flow cytometry core at the Department of Immunology, University of Pittsburgh for providing resources and expertise to perform ImageStream analysis (NIH 1S10OD019942-01, PI: Borghesi) as well as the Center of Biologic Imaging, University of Pittsburgh for providing resources to perform confocal imaging (Grant#1S10OD019973). The funders had no role in study design, data collection and analysis, decision to publish, or preparation of the manuscript.

DATA AVAILABILITY

The raw data that support the experimental findings are included as supplementary information. The image files used for computational analysis are uploaded at https://github.com/ankitbhatia/bioimage_aging. RNAseq data has been deposited to NCBI GEO database and is publicly available. The GEO accession number is GSE176478.

References

1. Conboy MJ, Conboy IM & Rando TA Heterochronic parabiosis: historical perspective and methodological considerations for studies of aging and longevity. Aging cell 12, 525–530, doi:10.1111/acel.12065 (2013). [PubMed: 23489470]
2. Conboy IM et al. Rejuvenation of aged progenitor cells by exposure to a young systemic environment. Nature. 433.(7027.):760.–4 (2005). [PubMed: 15716955]
3. Brack AS et al. Increased Wnt signaling during aging alters muscle stem cell fate and increases fibrosis. Science. 317.(5839.):807.–10 (2007). [PubMed: 17690295]
4. Sousa-Victor P et al. MANF regulates metabolic and immune homeostasis in ageing and protects against liver damage. Nat Metab 1, 276–290, doi:10.1038/s42255-018-0023-6 (2019). [PubMed: 31489403]
5. Li L et al. Impairment of chondrocyte proliferation after exposure of young murine cartilage to an aged systemic environment in a heterochronic parabiosis model. Swiss Med Wkly 148, w14607, doi:10.4414/smw.2018.14607 (2018). [PubMed: 29694646]
6. Gontier G et al. Tet2 Rescues Age-Related Regenerative Decline and Enhances Cognitive Function in the Adult Mouse Brain. Cell Rep 22, 1974–1981, doi:10.1016/j.celrep.2018.02.001 (2018). [PubMed: 29466726]
7. Pathan M et al. Vesiclepedia 2019: a compendium of RNA, proteins, lipids and metabolites in extracellular vesicles. Nucleic Acids Res 47, D516–D519, doi:10.1093/nar/gky1029 (2019). [PubMed: 30395310]
8. Shah R, Patel T & Freedman JE Circulating Extracellular Vesicles in Human Disease. N Engl J Med 379, 2180–2181, doi:10.1056/NEJMc1813170 (2018).
9. Chen WW et al. BEAMing and Droplet Digital PCR Analysis of Mutant IDH1 mRNA in Glioma Patient Serum and Cerebrospinal Fluid Extracellular Vesicles. Mol Ther Nucleic Acids 2, e109, doi:10.1038/mtna.2013.28 (2013). [PubMed: 23881452]

10. Yang J, Wei F, Schafer C & Wong DT Detection of tumor cell-specific mRNA and protein in exosome-like microvesicles from blood and saliva. PLoS One 9, e110641, doi:10.1371/journal.pone.0110641 (2014). [PubMed: 25397880]
11. Salih M, Zietse R & Hoorn EJ Urinary extracellular vesicles and the kidney: biomarkers and beyond. Am J Physiol Renal Physiol 306, F1251–1259, doi:10.1152/ajprenal.00128.2014 (2014). [PubMed: 24694589]
12. Monguio-Tortajada M et al. Extracellular-Vesicle Isolation from Different Biological Fluids by Size-Exclusion Chromatography. Curr Protoc Stem Cell Biol 49, e82, doi:10.1002/cpsc.82 (2019). [PubMed: 30698351]
13. Arraud N et al. Extracellular vesicles from blood plasma: determination of their morphology, size, phenotype and concentration. J Thromb Haemost 12, 614–627, doi:10.1111/jth.12554 (2014). [PubMed: 24618123]
14. Revenfeld AL et al. Diagnostic and prognostic potential of extracellular vesicles in peripheral blood. Clin Ther 36, 830–846, doi:10.1016/j.clinthera.2014.05.008 (2014). [PubMed: 24952934]
15. Valadi H et al. Exosome-mediated transfer of mRNAs and microRNAs is a novel mechanism of genetic exchange between cells. Nat Cell Biol 9, 654–659, doi:10.1038/ncb1596 (2007). [PubMed: 17486113]
16. Robbins PD Extracellular vesicles and aging. Stem Cell Investig 4, 98, doi:10.21037/sci.2017.12.03 (2017).
17. Alibhai FJ et al. Cellular senescence contributes to age-dependent changes in circulating extracellular vesicle cargo and function. Aging Cell 19, e13103, doi:10.1111/acel.13103 (2020). [PubMed: 31960578]
18. Yoshida M et al. Extracellular Vesicle-Contained eNAMPT Delays Aging and Extends Lifespan in Mice. Cell Metab 30, 329–342 e325, doi:10.1016/j.cmet.2019.05.015 (2019). [PubMed: 31204283]
19. Picca A et al. Mitochondrial Dysfunction and Aging: Insights from the Analysis of Extracellular Vesicles. Int J Mol Sci 20, doi:10.3390/ijms20040805 (2019).
20. Dubal DB et al. Life extension factor klotho enhances cognition. Cell Rep 7, 1065–1076, doi:10.1016/j.celrep.2014.03.076 (2014). [PubMed: 24813892]
21. Sahu A et al. Age-related declines in alpha-Klotho drive progenitor cell mitochondrial dysfunction and impaired muscle regeneration. Nat Commun 9, 4859, doi:10.1038/s41467-018-07253-3 (2018). [PubMed: 30451844]
22. Ahrens HE, Huettemeister J, Schmidt M, Kaether C & von Maltzahn J Klotho expression is a prerequisite for proper muscle stem cell function and regeneration of skeletal muscle. Skelet Muscle 8, 20, doi:10.1186/s13395-018-0166-x (2018). [PubMed: 29973273]
23. Tapscott SJ The circuitry of a master switch: Myod and the regulation of skeletal muscle gene transcription. Development 132, 2685–2695, doi:10.1242/dev.01874 (2005). [PubMed: 15930108]
24. Zammit PS et al. Pax7 and myogenic progression in skeletal muscle satellite cells. J Cell Sci 119, 1824–1832, doi:10.1242/jcs.02908 (2006). [PubMed: 16608873]
25. Zhang H et al. NAD(+) repletion improves mitochondrial and stem cell function and enhances life span in mice. Science 352, 1436–1443, doi:10.1126/science.aaf2693 (2016). [PubMed: 27127236]
26. Pala F et al. Distinct metabolic states govern skeletal muscle stem cell fates during prenatal and postnatal myogenesis. J Cell Sci 131, doi:10.1242/jcs.212977 (2018).
27. Paradies G, Paradies V, De Benedictis V, Ruggiero FM & Petrosillo G Functional role of cardiolipin in mitochondrial bioenergetics. Biochim Biophys Acta 1837, 408–417, doi:10.1016/j.bbabio.2013.10.006 (2014). [PubMed: 24183692]
28. Cecchini G Function and structure of complex II of the respiratory chain. Annu Rev Biochem 72, 77–109, doi:10.1146/annurev.biochem.72.121801.161700 (2003). [PubMed: 14527321]
29. Gamez-Valero A et al. Size-Exclusion Chromatography-based isolation minimally alters Extracellular Vesicles' characteristics compared to precipitating agents. Sci Rep 6, 33641, doi:10.1038/srep33641 (2016). [PubMed: 27640641]
30. Andreu Z & Yanez-Mo M Tetraspanins in extracellular vesicle formation and function. Front Immunol 5, 442, doi:10.3389/fimmu.2014.00442 (2014). [PubMed: 25278937]

31. Moon S et al. Enrichment of Exosome-Like Extracellular Vesicles from Plasma Suitable for Clinical Vesicular miRNA Biomarker Research. J Clin Med 8, doi:10.3390/jcm8111995 (2019).
32. Villeda SA et al. Young blood reverses age-related impairments in cognitive function and synaptic plasticity in mice. Nat Med 20, 659–663, doi:10.1038/nm.3569 (2014). [PubMed: 24793238]
33. Thery C et al. Minimal information for studies of extracellular vesicles 2018 (MISEV2018): a position statement of the International Society for Extracellular Vesicles and update of the MISEV2014 guidelines. J Extracell Vesicles 7, 1535750, doi:10.1080/20013078.2018.1535750 (2018). [PubMed: 30637094]
34. Mastoridis S et al. Multiparametric Analysis of Circulating Exosomes and Other Small Extracellular Vesicles by Advanced Imaging Flow Cytometry. Front Immunol 9, 1583, doi:10.3389/fimmu.2018.01583 (2018). [PubMed: 30034401]
35. Gualerzi A et al. Raman spectroscopy uncovers biochemical tissue-related features of extracellular vesicles from mesenchymal stromal cells. Sci Rep 7, 9820, doi:10.1038/s41598-017-10448-1 (2017). [PubMed: 28852131]
36. Movasaghi Z, Rehman S & Rehman IU Raman spectroscopy of biological tissues. Applied Spectroscopy Reviews 42 (2007).
37. de Cavanagh EA, Inserra F & Ferder L ANGIOTENSIN II BLOCKADE: HOW ITS MOLECULAR TARGETS MAY SIGNAL TO MITOCHONDRIA AND SLOW AGING. COINCIDENCES WITH CALORIE RESTRICTION AND mTOR INHIBITION. American journal of physiology. Heart and circulatory physiology, ajpheart.00459.02014, doi:10.1152/ajpheart.00459.2014 (2015).
38. Murphy E & Eisner DA Regulation of intracellular and mitochondrial sodium in health and disease. Circ Res 104, 292–303, doi:10.1161/CIRCRESAHA.108.189050 (2009). [PubMed: 19213964]
39. Brookes PS, Yoon Y, Robotham JL, Anders MW & Sheu SS Calcium, ATP, and ROS: a mitochondrial love-hate triangle. Am J Physiol Cell Physiol 287, C817–833, doi:10.1152/ajpcell.00139.2004 (2004). [PubMed: 15355853]
40. Garlid KD & Paucek P Mitochondrial potassium transport: the K(+) cycle. Biochim Biophys Acta 1606, 23–41, doi:10.1016/s0005-2728(03)00108-7 (2003). [PubMed: 14507425]
41. Garth J et al. The Effects of the Anti-aging Protein Klotho on Mucociliary Clearance. Front Med (Lausanne) 6, 339, doi:10.3389/fmed.2019.00339 (2019). [PubMed: 32039219]
42. Tang G, Shen Y, Gao P, Song SS & Si LY Klotho attenuates isoproterenol-induced hypertrophic response in H9C2 cells by activating Na(+)/K(+)-ATPase and inhibiting the reverse mode of Na(+)/Ca(2+)-exchanger. In Vitro Cell Dev Biol Anim 54, 250–256, doi:10.1007/s11626-017-0215-5 (2018). [PubMed: 29344767]
43. Shumilina E et al. Altered regulation of cytosolic Ca(2)(+) concentration in dendritic cells from klotho hypomorphic mice. Am J Physiol Cell Physiol 305, C70–77, doi:10.1152/ajpcell.00355.2012 (2013). [PubMed: 23596175]
44. Strutz-Seebohm N, Wrobel E, Schulze-Bahr E & Seebohm G Klotho: a new trafficking modifier of Kv7.1/KCNE1 channels. Channels (Austin) 8, 285, doi:10.4161/chan.29659 (2014). [PubMed: 25478618]
45. Ohnishi M & Razzaque MS Dietary and genetic evidence for phosphate toxicity accelerating mammalian aging. FASEB J 24, 3562–3571, doi:10.1096/fj.09-152488 (2010). [PubMed: 20418498]
46. Wehling-Henricks M et al. Klotho gene silencing promotes pathology in the mdx mouse model of Duchenne muscular dystrophy. Hum Mol Genet 25, 2465–2482, doi:10.1093/hmg/ddw111 (2016). [PubMed: 27154199]
47. Cheikhi A et al. Klotho: An Elephant in Aging Research. J Gerontol A Biol Sci Med Sci 74, 1031–1042, doi:10.1093/gerona/glz061 (2019). [PubMed: 30843026]
48. Gonzales PA et al. Large-scale proteomics and phosphoproteomics of urinary exosomes. J Am Soc Nephrol 20, 363–379, doi:10.1681/ASN.2008040406 (2009). [PubMed: 19056867]
49. Skog J et al. Glioblastoma microvesicles transport RNA and proteins that promote tumour growth and provide diagnostic biomarkers. Nat Cell Biol 10, 1470–1476, doi:10.1038/ncb1800 (2008). [PubMed: 19011622]

50. Zomer A et al. In Vivo imaging reveals extracellular vesicle-mediated phenocopying of metastatic behavior. Cell 161, 1046–1057, doi:10.1016/j.cell.2015.04.042 (2015). [PubMed: 26000481]
51. de la Cuesta F et al. Extracellular vesicle cross-talk between pulmonary artery smooth muscle cells and endothelium during excessive TGF-beta signalling: implications for PAH vascular remodelling. Cell Commun Signal 17, 143, doi:10.1186/s12964-019-0449-9 (2019). [PubMed: 31703702]
52. Kuro-o M et al. Mutation of the mouse klotho gene leads to a syndrome resembling ageing. Nature 390, 45–51, doi:10.1038/36285 (1997). [PubMed: 9363890]
53. Li S et al. exoRBase: a database of circRNA, lncRNA and mRNA in human blood exosomes. Nucleic Acids Res 46, D106–D112, doi:10.1093/nar/gkx891 (2018). [PubMed: 30053265]
54. Egerman MA et al. GDF11 Increases with Age and Inhibits Skeletal Muscle Regeneration. Cell metabolism 22, 164–174, doi:10.1016/j.cmet.2015.05.010 (2015). [PubMed: 26001423]
55. Choi JS et al. Exosomes from differentiating human skeletal muscle cells trigger myogenesis of stem cells and provide biochemical cues for skeletal muscle regeneration. J Control Release 222, 107–115, doi:10.1016/j.jconrel.2015.12.018 (2016). [PubMed: 26699421]
56. Eldh M et al. Exosomes communicate protective messages during oxidative stress; possible role of exosomal shuttle RNA. PLoS One 5, e15353, doi:10.1371/journal.pone.0015353 (2010). [PubMed: 21179422]
57. Fry CS, Kirby TJ, Kosmac K, McCarthy JJ & Peterson CA Myogenic Progenitor Cells Control Extracellular Matrix Production by Fibroblasts during Skeletal Muscle Hypertrophy. Cell Stem Cell 20, 56–69, doi:10.1016/j.stem.2016.09.010 (2017). [PubMed: 27840022]
58. Villarroya-Beltri C et al. Sumoylated hnRNPA2B1 controls the sorting of miRNAs into exosomes through binding to specific motifs. Nat Commun 4, 2980, doi:10.1038/ncomms3980 (2013). [PubMed: 24356509]
59. de Moura MB & Van Houten B Bioenergetic analysis of intact mammalian cells using the Seahorse XF24 Extracellular Flux analyzer and a luciferase ATP assay. Methods Mol Biol 1105, 589–602, doi:10.1007/978-1-62703-739-6_40 (2014). [PubMed: 24623254]
60. Zhang C et al. Arsenic Promotes NF-Kappab-Mediated Fibroblast Dysfunction and Matrix Remodeling to Impair Muscle Stem Cell Function. Stem Cells 34, 732–742, doi:10.1002/stem.2232 (2016). [PubMed: 26537186]

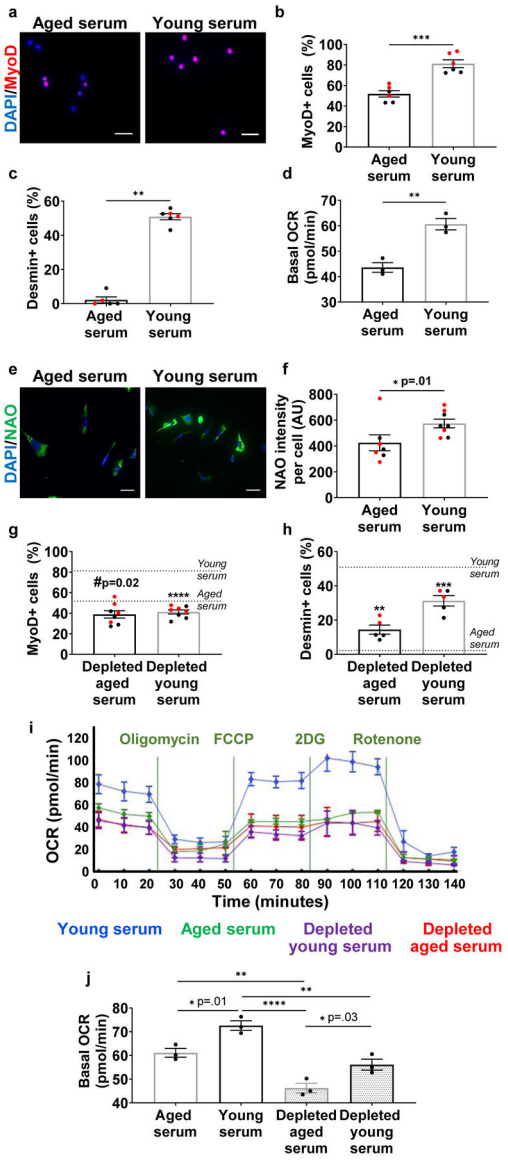

Fig. 1. The beneficial effect of young serum on aged muscle progenitors is dependent on circulating EVs

a, Immunofluorescent imaging of MyoD (red) and nuclei (DAPI; blue) in aged MPCs cultured with serum from aged or young mice. Scale: 25 μm. Quantification of **b,** MyoD and **c,** desmin (b: ***p < 0.0001, two-tailed Welch's t-test, n=6 wells/group. c: **p<0.01, two-tailed Mann-Whitney test, n=5 wells/group). **d,** Quantification of oxygen consumption rates (OCR) of MPCs cultured in the presence of aged or young serum. The experiment was repeated in triplicate. Data presented were taken from one representative experiment (**p<0.01, two-tailed Student's t test, 3–4 wells/group averaged over n=3 time points prior to oligomycin treatment). **e,** Immunofluorescent imaging and **f,** quantification of cardiolipin (NAO; green) and nuclei (DAPI; blue) in aged MPCs cultured with young or aged serum. Scale bar: 50 μm (*p < 0.05, two-tailed Mann Whitney test, n=7 (aged serum), 8 (young serum) wells). Quantification of **g,** MyoD (#p<0.05, ****p<0.0001 when compared to age-matched controls from figure 1B, two-tailed student's t-test, n=8 wells/group) and **h,** desmin

(**p<0.05, ***p<0.001 when compared to age-matched controls from figure 1c, two-tailed student's t-test, n=5 wells/group) in cells treated with young or aged serum depleted of EVs. **i,** Representative bioenergetic profiles of aged cells treated with young or aged serum with or without EVs (n=3 independent experiments). **j,** Seahorse analysis of aged MPCs treated with young and aged serum depleted of EVs (*p<0.05, **p<0.01, ****p<0.0001, one-way ANOVA with Tukey's multiple comparisons). Data presented as mean ± SEM of n=3 time points prior to oligomycin treatment, performed in 4–8 wells/group, as shown in figure 1i. The experiment was repeated in triplicate, and one experimental set of data is presented. Data are presented as mean ± SEM. Data from different cohorts or experimental groups performed on different days are presented within the same graph as black or red circles.

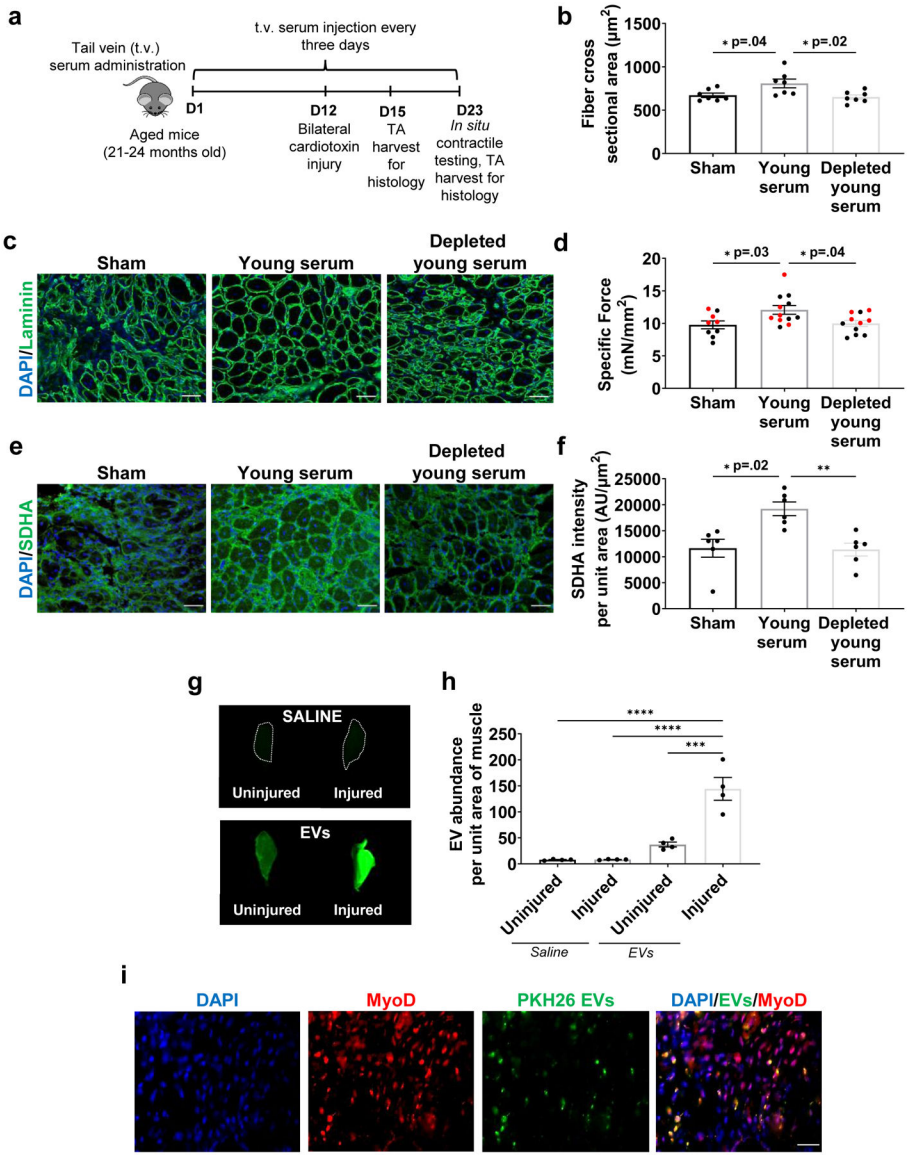

Fig. 2. The beneficial effect of young serum on aged muscle regeneration and mitochondrial function is dependent, at least in part, on circulating EVs.

a, Schematic of the experimental paradigm for muscle functional recovery after serum injections. **b**, Quantification and **c**, representation of cross-sectional area of muscle fibers (Laminin; green) and nuclei (DAPI; blue). Scale: 50 μm. (*p<0.05, n=7/group, one-way ANOVA with Tukey's multiple comparisons). **d**, Comparison of peak specific force across the three experimental groups (*p<0.05, n=9 (Sham), 11 (Young serum), 12 (Depleted young serum), one-way ANOVA with Tukey's multiple comparisons). **e**, Representation and **f**, quantification of SDHA in regenerating myofibers of injured muscles receiving sham, young serum, or EV-depleted young serum treatments. (SDHA; green) and nuclei (DAPI; blue) (*p<0.05, **p<0.01, n=6/group, non-parametric ANOVA with Dunn's multiple comparisons). **g**, LiCOR imaging and **h**, quantification of intensity of labeled EVs in uninjured and injured TAs receiving saline or dyed EVs in the circulation. The experiment was repeated in duplicate. **i**, Quantification of intensity of labeled EVs in muscle using

scanned images of TA muscles by LiCOR Odyssey equipment. (****p<0.0001, one-way ANOVA with Tukey's multiple comparisons, n=4/group). **i**, Representative image of MyoD+ cells co-localizing with PKH26 dyed EVs at the site of injury 48 hours after EV injection. The immunofluorescence staining was repeated in duplicate by two independent investigators. Scale: 25 μm. Data presented as mean ± SEM. Data from different cohorts or experimental groups performed on different days are presented within the same graph as black or red circles.

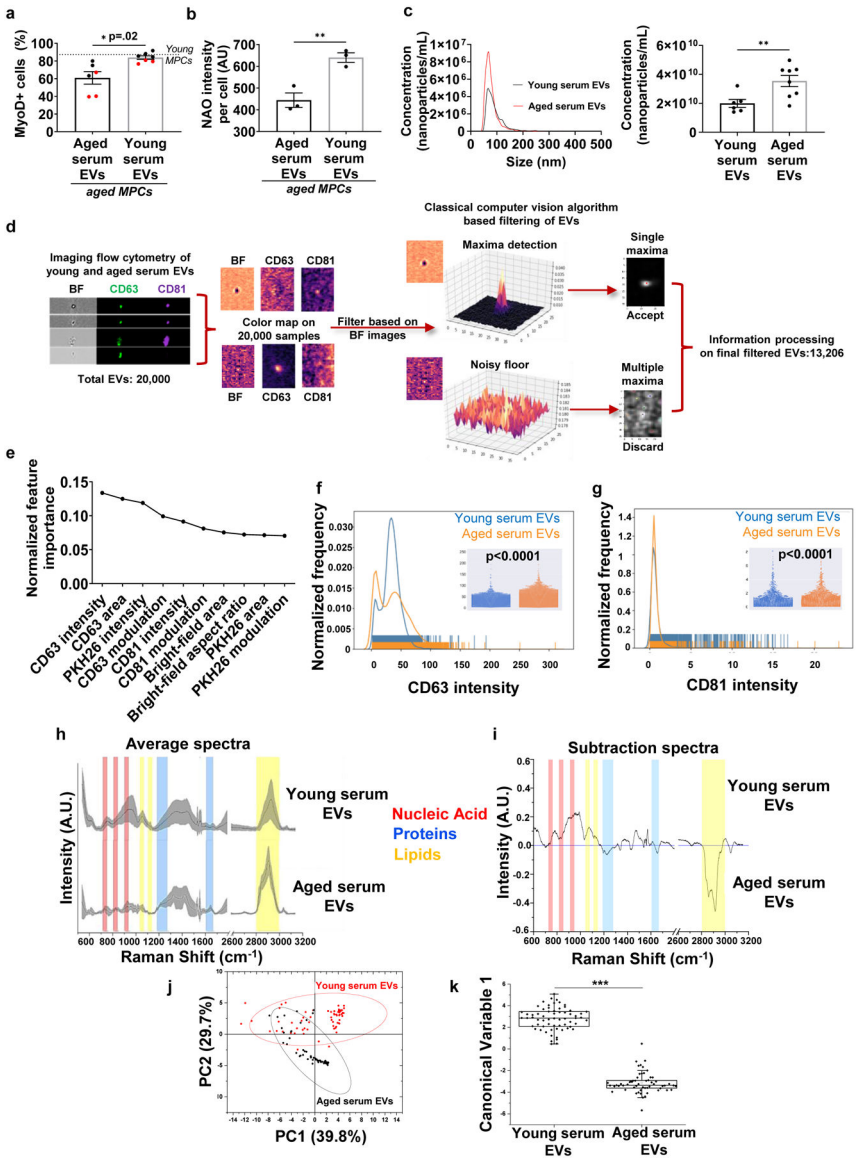

Fig. 3. Aging shifts EV subpopulation heterogeneity and disrupts the biochemical fingerprint of EVs.

a, Quantification of MyoD-positive aged MPCs treated with young or aged serum EVs (*p<0.05, two-tailed Welch's t-test, n=6 (Aged),7(Young) wells). **b,** Quantification of cardiolipin content (NAO) of aged MPCs following exposure to young or aged EVs (**p<0.01, two-tailed Student's t-test, 3 wells/group, data representative of two independent experiments). **c,** Representative histogram and quantification of nanoparticle concentration in young and aged serum EVs (**p<0.01, two-tailed Welch's test, n=6 (Young), 8 (Aged) samples). **d,** Classical computer vision-based filtering of imaging flow cytometry images of EVs based on the bright-field channel. **e,** Elbow plot of gradient-boosted decision tree classifier derived feature importance ranks to discriminate EVs based on age. Features used were based on size (area, aspect ratio), signal strength (intensity) and texture (modulation) of the EVs in the bright-field, CD63, CD81 and PKH26 image channels. Rug plots and beeswarm plots (inset) for **f,** CD63 intensity (p<0.0001, n=6417–13077 EVs per group

for this experimental run, EVs pooled from 4 serum samples of both young and aged animals, two-tailed Mann Whitney test, experiment repeated in triplicates) and **g,** CD81 intensity for young and aged serum EVs. ($p<0.0001$, n=6417 (young),13077 (aged) EVs for this experimental run, EVs pooled from 4 serum samples of both young and aged animals, two-tailed Mann Whitney test, experiment repeated in triplicates). **h,** Average Raman spectra with standard deviation (grey band) of young and aged serum EVs. **i,** Subtraction spectrum of the differences between the average spectra acquired for young and aged serum EVs. **j,** Principal Component Analysis (PCA) with 95% confidence interval and **k,** Linear Discriminant Analysis of spectra data acquired from aged and young serum EVs (n=5 samples/group; ***$p<0.001$, two-tailed Mann Whitney test). Minima, maxima, median, 25^{th} percentile and 75^{th} percentile: 0.46324, 5.082, 2.85669, 2.09799, 3.45523 (young serum EVs); −5.67133, 0.48193, −3.35317, −3.60656 and −2.9319 (aged serum EVs). Boundaries determined using inter-quartile range with 1.5 as coefficient: 1.35723 for young serum EVs and 0.67466 for aged serum EVs.

Data presented as mean ± SEM.

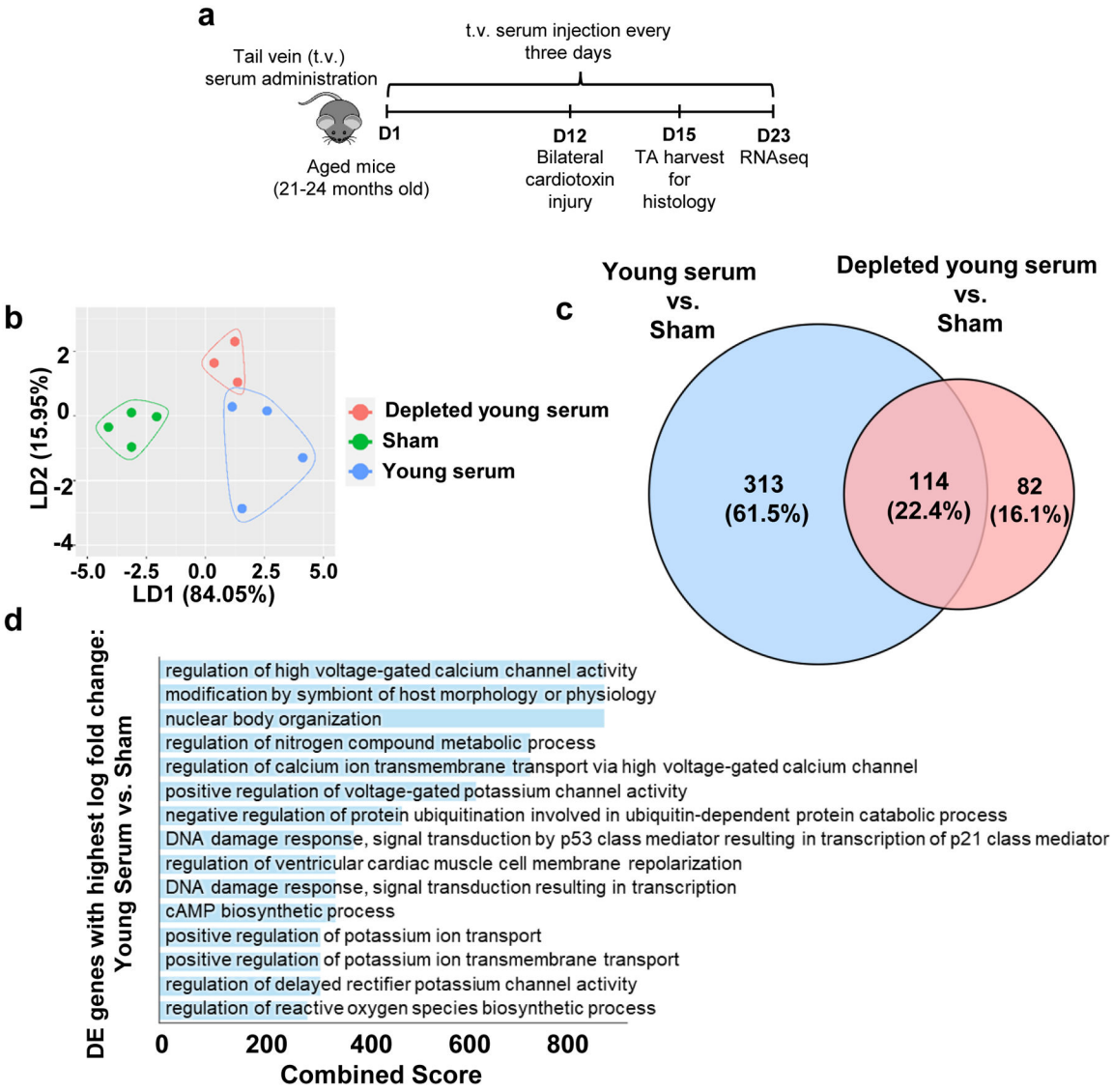

Fig. 4. Transcriptomic alterations in skeletal muscle with young serum treatment are predominated by EVs.

a, Schematic of the experimental paradigm for RNAseq analyses after serum injections. **b,** Linear Discriminant Analysis (LDA) of RNA-seq data acquired from injured aged skeletal muscles receiving sham, young serum, or EV-depleted young serum injections. **c,** Venn diagram displaying overlap of global differentially expressed (DE) genes when comparing young serum vs. sham and EV-depleted young serum vs. sham (Log fold change magnitude 0.1, false discovery rate magnitude 0.1). **d,** Gene ontology (GO) terms for highly differentially expressed due to the presence of EVs in young serum (log fold change magnitude higher than 1.5, false discovery rate magnitude lesser than 0.1).

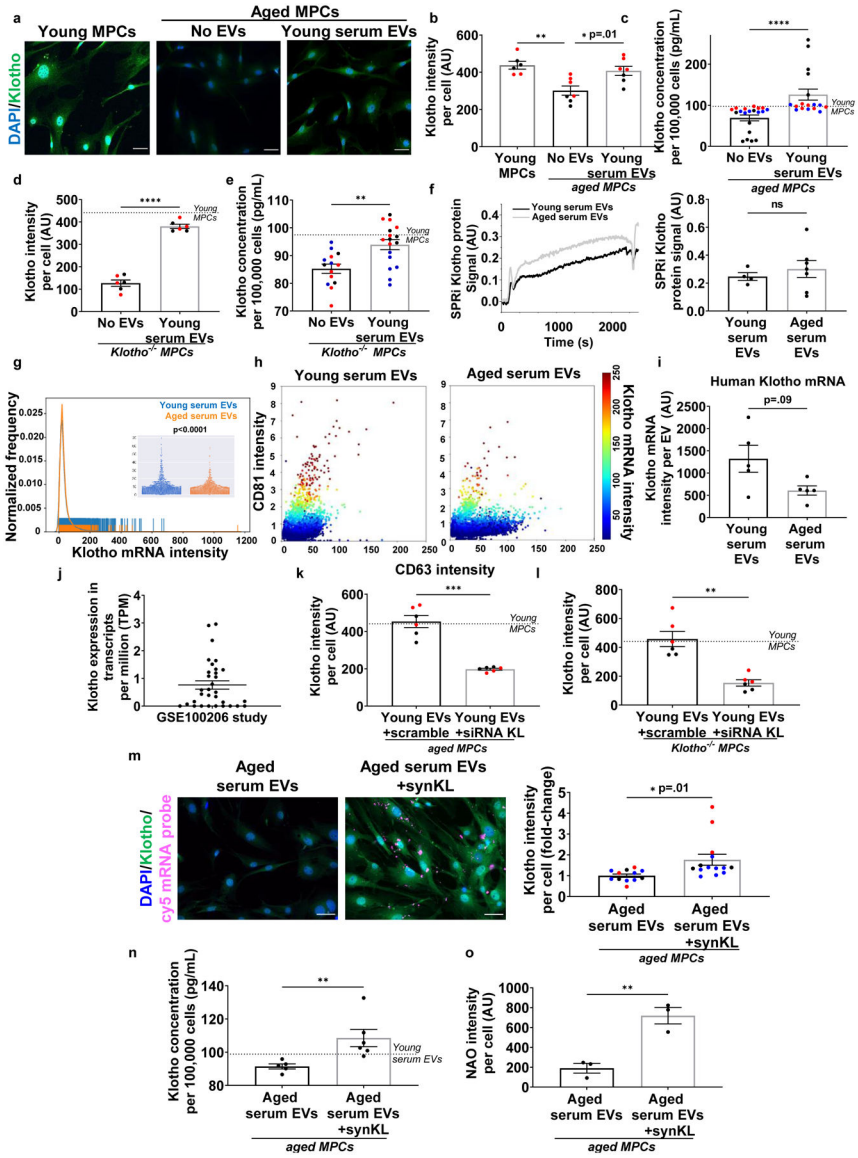

Fig. 5. Klotho transcripts in EVs decline over time and are preferentially contained within EVs with high expression of the CD81 surface marker.

a, Imaging and **b**, quantification of Klotho (green) in MPCs cultured in the presence or absence of young EVs in culturing media. Scale bar: 50 μm. (*p<0.05, **p<0.01, one-way ANOVA with Tukey's multiple comparisons, n= 6 (Young MPCs), 7 (No EVs), 7 (Young serum EVs) wells). **c**, Quantification of secreted Klotho in conditioned media of aged MPCs treated with or without young EVs (****p < 0.01, two-tailed Mann Whitney test, n=11 (No EVs), 20 (Young serum EVs)). **d**, Klotho quantification in Klotho$^{-/-}$ MPCs in the presence of no EVs or young EVs (****p<0.0001, two-tailed Welch's t-test, n=6 wells/group). **e**, Quantification of secreted Klotho in culture media of Klotho$^{-/-}$ MPCs in the presence or absence of young EVs (***p<0.001, two-tailed Welch's test, n=14 (No EVs), 17 (Young serum EVs)). **f,** Surface Plasmon Resonance imaging (SPRi) and analysis of Klotho protein in young and aged serum EVs. (p>0.05, two-tailed Student's t test, n=4 (Young), 7(Aged)). **g**, Rug plot with beeswarm plot of Klotho mRNAs in young and aged serum EVs. **h**,

3D-plots of Klotho mRNA distribution in CD63 and CD81 positive circulating EVs. **i**, Klotho mRNAs quantification in young and aged human serum EVs. ($p>0.05$, two-tailed Welch's t-test, n=5/group) **j**, Human EV-Klotho mRNA quantification in publicly archived dataset (n=32). **k**, Klotho quantification in aged MPCs receiving young EVs treated with either non-targeting siRNA (scramble) or siRNA to *Klotho* (***$p<0.001$, two-tailed Welch's t-test, n=6 wells/group, repeated in two independent experiments). **l**, Klotho quantification in $Kl^{-/-}$ MPCs receiving young EVs treated either with a non-targeting siRNA (scramble) or siRNA to *Klotho* (***$p<0.001$, two-tailed Welch's t-test, n=6 wells/group, repeated in two independent experiments). **m**, Imaging and quantification of Klotho protein (green) in aged MPCs receiving aged EVs engineered with synthetic Klotho mRNA (pink). Scale: 50 μm. (*$p<0.05$, two-tailed Welch's t-test, n=12 (aged EVs), 14 (aged EVs+synKL) wells, presented as fold change over aged serum EVs per experiment). **n**, Klotho quantification in conditioned media of aged MPCs administered with aged EVs or aged EVs engineered with synthetic Klotho mRNA (**$p<0.01$, two-tailed Student' t test, n=5 (aged EVs), 6 (aged EVs+synKL)). **o**, Cardiolipin (NAO) quantification in aged MPCs treated with aged EVs or aged EVs engineered with synthetic mRNA (**$p<0.01$, two-tailed Mann Whitney test, n=3 wells/group, data representative of one of the two independent experiments). Data presented as mean ± SEM and different cohorts performed on different days presented within the same graph as black, red, or blue circles.

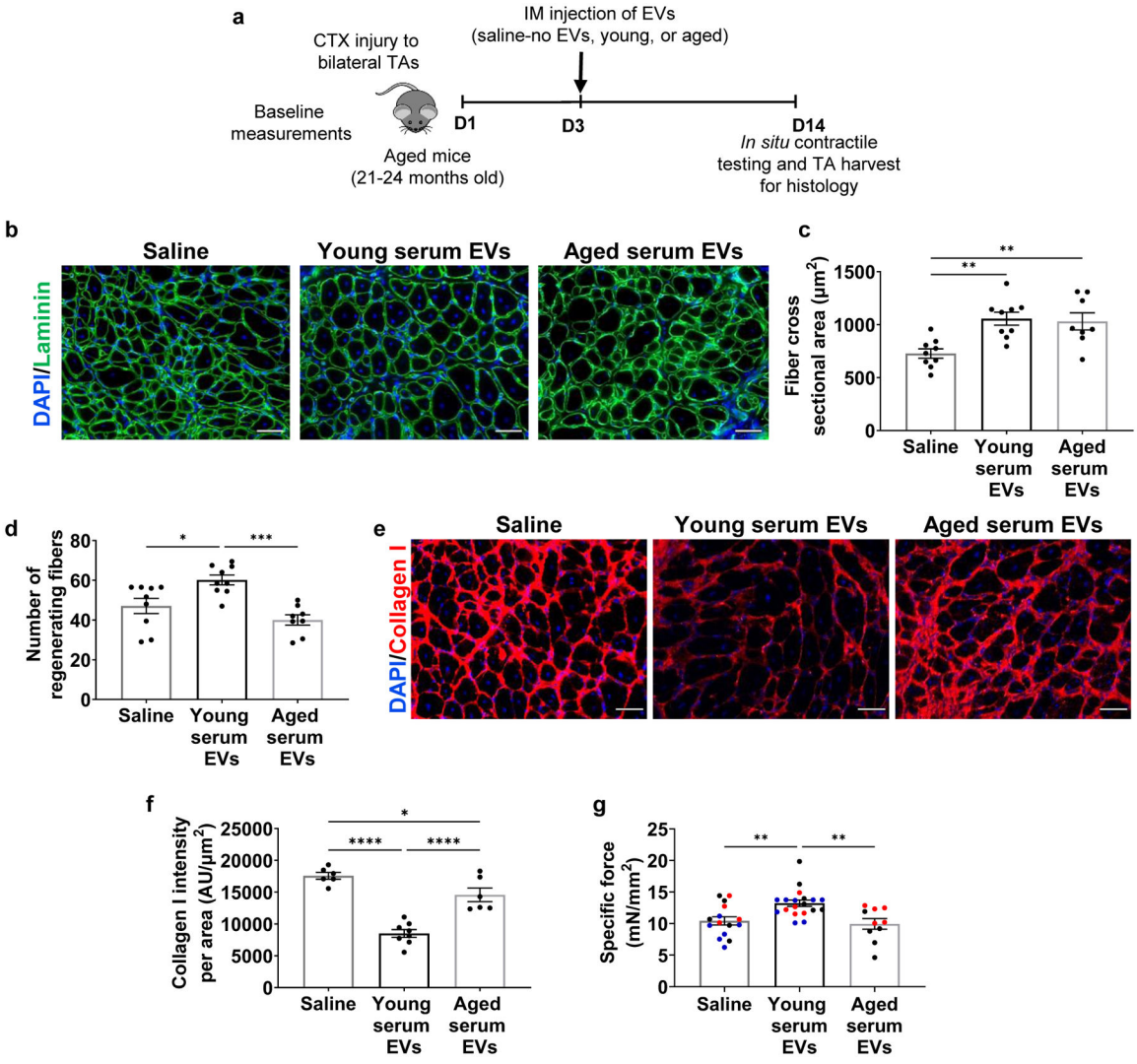

Fig. 6. EV age impacts skeletal muscle regeneration and function.

a, Schematic of the *in vivo* administration of EVs to injured aged mice. **b,** Representative images of laminin (green) and **c,** histological analysis of fiber cross-sectional area of injured TAs of aged mice receiving saline, young, or aged EVs. (**p<0.01, one-way ANOVA with Tukey's multiple comparisons, n=8–9/group). Scale: 50 μm. **d,** Quantification of number of regenerating fibers in injured TAs of aged mice receiving saline, young serum EVs, or aged serum EVs (***p<0.001, *p<0.01, one-way ANOVA with Tukey's multiple comparisons, n=8 (aged), 9 (saline, young)). **e,** Representative images of Collagen I in injured muscle cross-sections of aged mice receiving saline, young, or aged EVs. **f,** Histological analysis of Collagen I in injured muscle cross-sections of aged mice receiving young or aged EVs when compared to saline-injected controls (*p<0.05, ****p<.0001, one-way ANOVA with Tukey's multiple comparisons, n=6 (saline, aged), 8 (young)). Scale: 50 μm. **g,** Specific tetanic force of aged animals receiving intramuscular injections of saline, young, or aged EVs. (**p<0.01, one-way ANOVA with Tukey's multiple comparison, n=10 (aged), 15 (saline), 19 (young)). Data presented as mean ± SEM. Data from different cohorts or

experimental groups performed on different days are presented within the same graph as black, blue, or red circles.

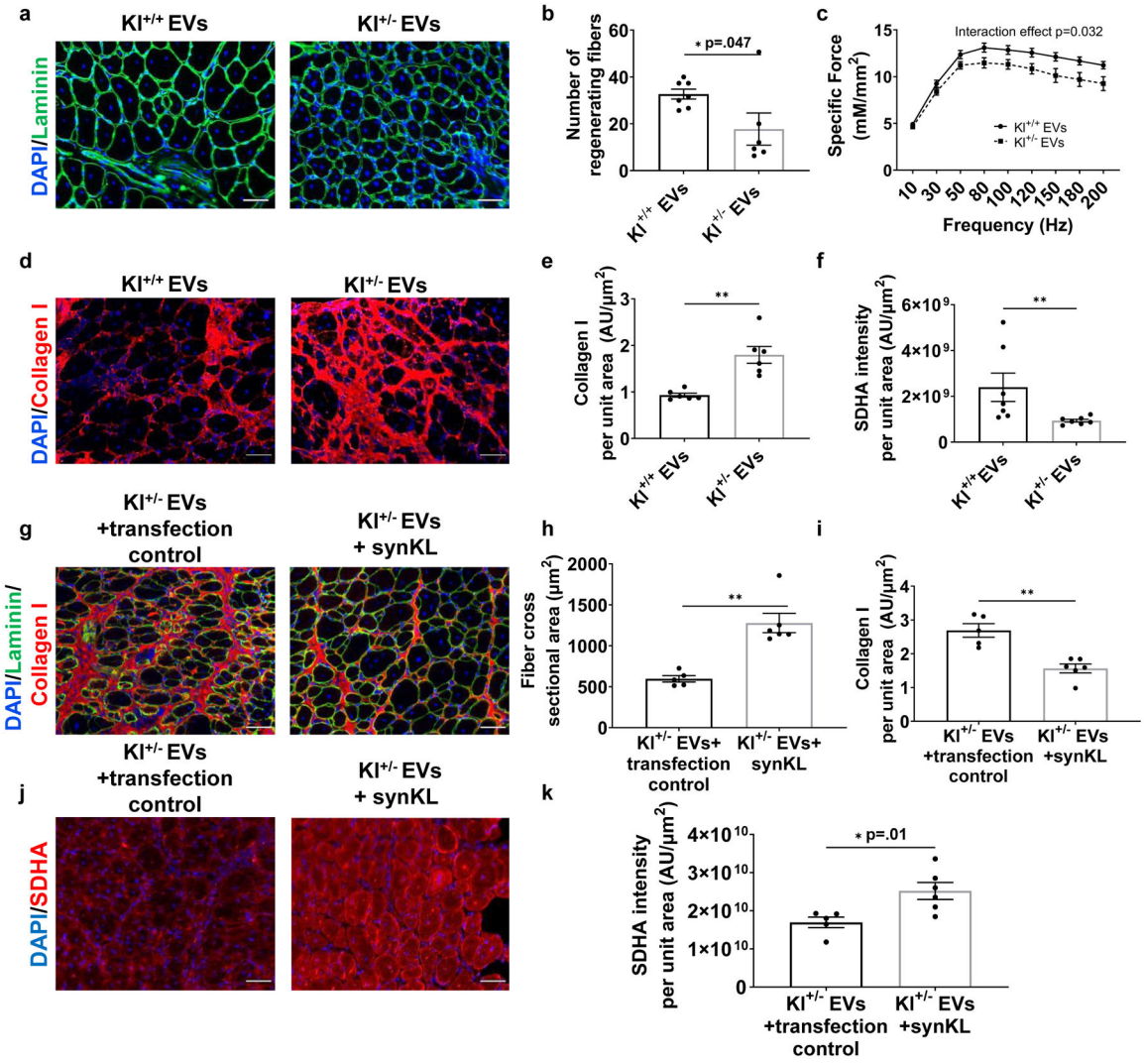

Fig. 7. Klotho mRNA within EVs contribute to functional skeletal muscle regeneration.

a, Representative images of fibers (Laminin) of injured aged TAs receiving Klotho$^{+/+}$ or Klotho$^{+/-}$ serum EVs. Scale: 50 µm. **b**, Number of regenerating fibers greater than 600µm^2 in injured TAs of aged mice receiving Klotho$^{+/+}$ or Klotho$^{+/-}$ serum EVs. (*p<0.05, two-tailed Mann Whitney test, n=6 (Kl$^{+/-}$), 7 (Kl$^{+/+}$)). **c**, Specific tetanic force frequency curves of aged animals receiving EVs isolated from Klotho$^{+/+}$ or Klotho$^{+/-}$ serum (two-way mixed ANOVA, repeated measures with frequency, interaction effect of frequency and experimental group p=0.032, n=18 (Kl$^{+/+}$), 20(Kl$^{+/-}$)). **d**, Representative images of Collagen I in injured muscles of aged mice receiving Klotho$^{+/+}$ or Klotho$^{+/-}$ serum EVs. Scale: 50 µm. **e**, Quantification of Collagen I in injured muscle cross-sections of aged mice receiving Klotho$^{+/+}$ or Klotho$^{+/-}$ serum EVs. (**p<0.01, two-tailed Welch's t-test, n=6/group). **f**, Quantification of SDHA of regenerating myofibers in injured TAs of aged mice receiving Klotho$^{+/+}$ or Klotho$^{+/-}$ serum EVs. (**p<0.01, two-tailed Mann Whitney test, n=7/group). **g**, Representative images and histological analysis of **h**, fiber cross-sectional area and **i**, collagen I of injured TAs of aged mice receiving Klotho$^{+/-}$ serum EVs loaded with transfection control or synthetic Klotho mRNA. (h: **p<0.01, two-tailed Mann Whitney

test; i: **p<0.01, two-tailed Mann Whitney test; n=5 ($Kl^{+/-}$ EVs+transfection control), 6 ($Kl^{+/-}$ EVs+ synKL)). Scale: 50 μm. **j**, Imaging and **k**, quantification of SDHA in regenerating myofibers at the site of injury receiving $Klotho^{+/-}$ serum EVs loaded with transfection control or synthetic Klotho mRNA. (*p<0.05, two-tailed Welch's t-test, n=5 ($Kl^{+/-}$ EVs+transfection control), 6 ($Kl^{+/-}$ EVs+ synKL)). Data presented as mean ± SEM.